JOURNAL OF PROPULSION AND POWER
Vol. 24, No. 3, May–June 2008

Resonance Frequencies and Damping of a Combustor Acoustically Coupled to an Absorber

Michael Oschwald* and Zoltán Faragó†
DLR, German Aerospace Center, 74239 Hardthausen, Germany
and
Geoff Searby‡ and François Cheuret§
Centre National de la Recherche Scientifique and Aix-Marseille Université, 13384 Marseille, France

DOI: 10.2514/1.32313

The coupled acoustic system of a cylindrical combustor and an absorber cavity has been investigated experimentally in hot-fire and cold-flow tests. The addition of an absorber volume to the combustor is shown to result in eigenfrequencies of the coupled system systematically different from that of a pure cylindrical resonance volume. The general behavior of the coupled system is explained based on an analytical one-dimensional analysis of the problem. Numerical simulations in two dimensions result in very good agreement with experimental observations. A three-dimensional simulation of a cylinder equipped with 40 absorbers demonstrates the relevance of the reported phenomena for rocket engines equipped with absorber rings. Experimental data on the damping behavior of an absorber are given and the damping of absorbers is discussed based on the numerically obtained acoustic eigenmodes of the coupled system.

Nomenclature

A	=	section of cavity or chamber, m^2
c	=	speed of sound, $m\,s^{-1}$
f	=	frequency, s^{-1}
k	=	acoustic wave number, m^{-1}
L	=	length of cavity or chamber, m
p	=	acoustic pressure, Pa
R	=	radius of cavity or chamber, m
S	=	ratio of cavity cross sections
T	=	ratio of cavity lengths
u	=	acoustic velocity, ms^{-1}
$\alpha_{n,m}$	=	abscissa of mth extremum of Bessel function of order n
Γ	=	full linewidth at half-height, s^{-1}
γ	=	nondimensional admittance
ρ	=	density, $kg\,m^{-3}$
ω	=	angular frequency, s^{-1}

Subscripts

1	=	main cavity
2	=	damping cavity
A	=	absorber
C	=	combustor
QW	=	quarter wave

Introduction

THE origin and control of high-frequency instability in liquid-fueled rocket engines is still an open problem. The interaction of acoustic eigenmodes of combustion chambers with the combustion processes can lead to severe anomalies of rocket motor performance [1,2]. Various methods have been used to increase the dissipation rate of acoustic disturbances in rocket engine combustion chambers so as to increase the stability margin of the motor. Baffles protruding into the combustor are applied to impose specific symmetries into the acoustic system that are not compatible with the symmetry of the eigenmode favored by the coupling mechanism. A prominent example in which baffles were used to stabilize a combustion chamber was the F-1 motor, the booster engine of the Saturn rocket [3]. Tuning of the injector's dynamic behavior is an elegant technique to suppress injection-coupled responses [4,5]. Acoustic cavities such as Helmholtz or quarter-wave resonators are used as damping devices in combustion systems like gas turbines and rocket combustors [6–8].

The design concept of a quarter-wave resonator is to tune its eigenfrequency to the eigenfrequency of the combustor. The quarter-wave cavity is behaving as a half-open resonator, its eigenfrequency is tuned by adjusting its length L according to

$$f_A = \frac{c}{4L} \tag{1}$$

(corrections of the mass accelerated by the acoustic field outside the resonator, as expressed by a correction ΔL of the cavity length are neglected).

The eigenfrequencies of combustion chambers can be approximated by the eigenmodes of cylinders, an approximation which is good enough for the discussions and analysis presented in this work. In the frame of linear acoustics, the eigenfrequencies of the transverse eigenmodes of a cylinder of radius R are [1]

$$f_C = \alpha_{nm}\frac{c}{2\pi R} \tag{2}$$

where α_{nm} is the abscissa of the mth extremum of the Bessel function of the first kind of order n. For a tuned cavity, $f_A = f_C$ and thus the length of the "tuned" absorber is

$$L = \frac{\pi R}{2\alpha_{nm}} \tag{3}$$

For the first tangential mode, $\alpha_{11} = 1.841$, resulting in a tuned cavity when

Received 24 May 2007; revision received 21 November 2007; accepted for publication 24 November 2007.

*Head Rocket Propulsion, Lampoldshausen, Langer Grund.
†Research Scientist, Lampoldshausen, Langer Grund.
‡Senior Scientist, Institut de Recherche sur les Phénomènes Hors Équilibre, 49 rue Joliot-Curie.
§Ph.D. Student, Institut de Recherche sur les Phénomènes Hors Équilibre, 49 rue Joliot-Curie.

$$L = 0.8532 \cdot R \tag{4}$$

When this criterion is used to tune a quarter-wave cavity to the eigenfrequency of the combustion chamber, it is expected that the cavity will have a maximal response with strong acoustic velocity oscillations at the cavity inlet. These velocity oscillations dissipate acoustic energy, both through viscous losses at the cavity walls and also through vortex generation and turbulent dissipation at the cavity exit. The absorber tube thus enhances the damping of the excited eigenmode.

In practice, the tuning of absorbers is not as straightforward as the preceding sketch, and the applications of $\lambda/4$ cavities does not always result in the expected performance. Several reasons are usually put forward to explain these difficulties. In hot-fire conditions, there is a temperature gradient along the absorber axis, the sound velocity therefore is not constant. Because the temperature profile in general is not known exactly, a priori, tuning of the resonator to a specific frequency is difficult. Another difficulty results from the transient conditions during engine startup. The gas composition and temperature in the combustor, and also in the absorber, evolve rapidly during this transient period and thus the sound velocity, i.e., the resonance frequencies of the system, also vary. It is therefore not surprising that deviations from the expected resonance behavior are observed experimentally, and may be explained by these thermal and transient conditions.

However, to identify the influence of the temperature and gas composition, it is necessary to have an exact knowledge of the resonance behavior of the acoustic system. In this paper, we show that the presence of damping cavities can profoundly modify both the structure and frequency of the acoustic modes of combustion chambers. In particular, we will show that tuning an absorber according to Eq. (3) does not result in an optimal matching of the acoustic eigenfrequencies of the system, nor in optimal damping of the eigenmodes, even for the simple case of constant composition and temperature.

Results obtained during experimental investigations into the mechanisms leading to high-frequency combustion instabilities of O_2/ethanol-spray combustion [9] motivated a study to address the physics of the coupling of an absorber cavity to a combustor volume in more detail. In these hot-fire tests, it was observed that the resonance frequencies of the combustor were detuned when a secondary lateral nozzle was added to the cylindrical combustion chamber, see Fig. 1. Although, in these experiments, the additional volume was added to the combustor to allow siren-wheel acoustic excitation, the basic acoustical problem appeared to be very similar to that of a quarter-wave cavity coupled to a combustion chamber. The sonic throat of the secondary nozzle behaves like a closed end of a resonator tube, and thus the resonance conditions are similar to that of a $\lambda/4$ cavity. For this reason, the findings in the experiments with siren excitation has motivated an extended investigation of the acoustics of resonance tubes coupled to cylindrical volumes.

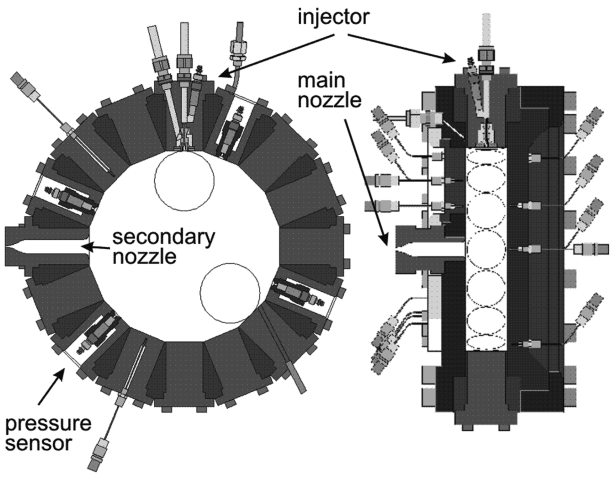

Fig. 1 Cross sections of the CRC.

In this paper, we show that the presence of cavities at the periphery of a combustion chamber profoundly modify the acoustic mode structure and resonance frequencies of a combustion chamber. The specific characteristics of the eigenmodes of the coupled acoustic system are discussed in terms of their resonance frequencies, their symmetry properties, and their damping behavior. The key parameter in this investigation is the length of the absorber L which is varied over a large range, including the specific cases $L = 0$ (a cylinder with no absorber) and $L/R = \pi/(2\alpha_{nm})$ (a cylinder with an absorber tuned to be quarter-wave resonant at the frequency of one of the transverse modes).

We start with a simple example of a cylindrical combustion chamber equipped with a single lateral cavity to demonstrate this behavior experimentally in hot-fire and cold-flow tests. The results show that the system is no longer resonant on the eigenmodes of the cylindrical chamber but has its own acoustic modes and, in general, these modes are quite different from those of the individual components.

To gain qualitative understanding, we then consider an idealized geometry of two rectangular cavities and calculate its eigenmodes analytically. This simple calculation provides insight into the general trends of the effect of a lateral cavity.

We then model the experimental cavity numerically, and show how the eigenfrequencies and mode shapes evolve with the geometry of the damping cavity. Finally, we show that the absorber admittances can be evaluated from the numerically predicted eigenmodes, and that these admittances can be used to predict damping efficiency and optimal tuning of cavities. These predictions are then compared with experimentally determined damping behavior of individual modes.

Test Setup

Common Research Chamber

For experiments with two types of propellants, O_2/ethanol and LOX/H2, two combustion chambers of similar design are used in our laboratories. This common research chamber (CRC) has a cylindrical shape with a radius of $R = 10$ cm. The frequencies of the tangential eigenmodes in hot-fire tests are in a range ($1T \sim 4$ kHz) representative of full-scale engines. The length of the chamber is 4 cm and, as a consequence, the longitudinal modes have eigenfrequencies far above the frequencies of the tangential modes of interest in these experiments.

The chamber is shown in Fig. 1. Sixteen ports in the cylindrical wall of the combustor can be equipped with various sensors or specific hardware. In one port, a coaxial injector head for ethanol/O_2 or for LOX/H2 can be mounted. In the latter case, the injector head is cooled with liquid N_2 to guarantee stationary thermal conditions during the transient injection startup of LOX. In respect to the disklike combustor volume and the radial injection of the propelants, the concept of the setup is similar to that used by Heidmann [10].

The exhaust gases are released through a main nozzle in the axial direction. Using nozzles with different throat diameters, and adjusting the mass flows, tests can be done at pressures between 1.5 and 10 bar. In one of the ports, a secondary nozzle can be mounted with a throat of 2 mm diameter. Depending on the main nozzle diameter, the ratio of throat area of the main nozzle to the secondary nozzle varies between 6 and 25. Pressures are measured with both static and dynamic pressure sensors. The number of available ports make it easy to place the pressure sensors in the required positions with respect to the symmetry of the acoustic mode of interest.

Hot-Fire Tests

The hot-fire tests in the CRC discussed in this report were done using liquid ethanol and gaseous oxygen as substitute fluids. The propellants were injected using a single coaxial injector with no recess. The internal and external diameters of the liquid post were 1.2 and 1.8 mm, respectively. The external diameter of the gas annulus was 2.5 or 3.0 mm. To avoid soot formation, the combustion chamber was run under lean to stoichiometric conditions. The mass

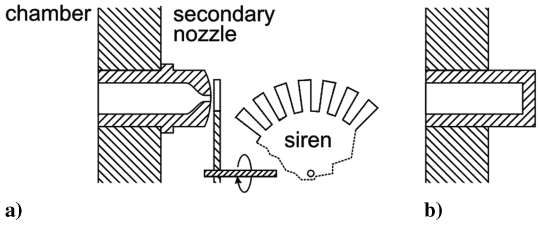

Fig. 2 Sketch of a) secondary nozzle and siren wheel used for acoustic excitation of the combustion chamber, and b) a quarter-wave cavity.

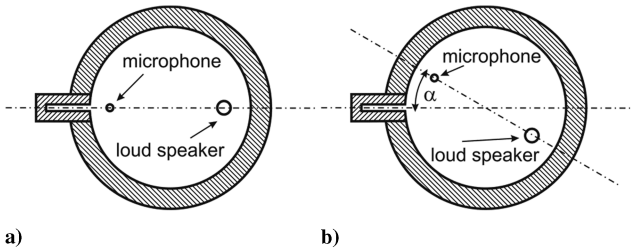

Fig. 3 Position of microphone and loudspeaker in the cold-flow tests.

flow rate of ethanol was in the range of 1.0–2.5 g/s, and that of oxygen was 4.8–7.0 g/s. The range of stoichiometry was 0.3–1.0. The injection velocity of the liquid ethanol was in the range of 2.5–6.3 m/s, and that of gaseous oxygen was 100–330 m/s.

A secondary nozzle, with a throat small compared to that of the main nozzle, could be placed in one of the access ports of the CRC, as shown in Figure 1. For some measurements, the CRC was acoustically excited by modulating the exhaust flow through the throat of this secondary nozzle, using a rotating toothed wheel placed immediately downstream, as sketched in Fig. 2a. The flow through the throat was periodically blocked by successive teeth, leading to acoustic excitation of the CRC. The speed of rotation of the disk could be controlled so as to excite the CRC at the desired resonant frequency. In general, the frequency was ramped at a low rate so as to sweep through the linewidth of the chosen resonance. The inlet of the secondary nozzle forms a lateral cavity with an internal diameter of 32 mm. The design allows the variation of the cavity length. The sonic throat of the secondary nozzle behaves like the closed end of a resonator, and thus the resonance conditions are similar to that of a quarter-wave cavity, as sketched in Fig. 2b.

Cold-Flow Tests

In hot-fire tests, there is interaction of the combustion process with the acoustic field and the species and temperature distributions in the combustor are not homogeneous. To allow acoustic measurements at well-defined conditions, the eigenfrequencies and damping coefficients of modes have been measured under cold-flow conditions. For this purpose, the CRC was filled with ambient air. A loudspeaker and a microphone were mounted in the front plate for acoustic excitation and for detecting the acoustic pressure oscillations in the chamber, respectively. If not stated otherwise, the loudspeaker and the microphone were positioned on a line at an angle of $\alpha = 0$ deg relative to the symmetry axis of the absorber, as shown in Fig. 3a. For specific objectives the angle α can be adjusted (see Fig. 3b).

Acoustic oscillations in the chamber have been excited in two different ways. In the first case, a white noise signal is sent to the loud speaker, and all resonances of the acoustic system are excited simultaneously, with the exception of modes having a pressure nodal line on the axis of the loudspeaker. In the second case, the chamber is excited with a preset single frequency using a frequency generator. For both methods, it has been proved that the measured resonance frequency and the damping characteristics of a given mode are the same. The white noise method yields a faster global analysis, whereas the single line excitation provides a much better signal-to-noise ratio.

To introduce the desired acoustic excitation in the CRC, the loudspeaker is switched on. The acoustic amplitude in the chamber first increases and then saturates at some constant amplitude. The loudspeaker is then switched off and the decay of the acoustic excitation is recorded (see Fig. 4).

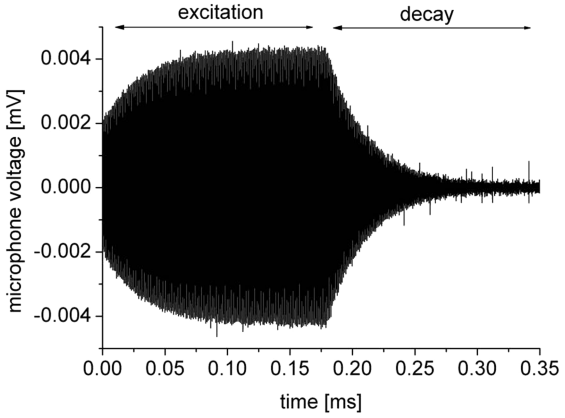

Fig. 4 Acoustic pressure during excitation of 1T resonance and decay of signal after shutoff of loudspeaker.

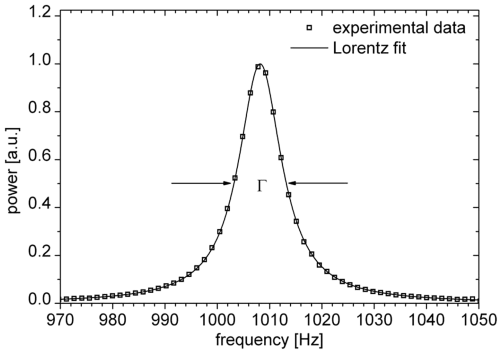

Fig. 5 Fourier transform of decaying acoustic pressure.

The differential equation

$$\ddot{p}' + \Gamma\dot{p}' + \omega_0^2 p' = 0 \tag{5}$$

describes the temporal evolution of a damped harmonic pressure oscillation. For small damping, the solution is [11]

$$p'(t) = p'_0 \cos(\omega_0 t) \exp\left(-\frac{\Gamma}{2}t\right) \tag{6}$$

The power spectrum $I(\omega)$ of the decaying pressure signal has a Lorentzian profile centered at the resonance frequency ω_0 [12]:

$$I(\omega) \propto p_0'^2 \frac{1}{(\omega - \omega_0)^2 + (\Gamma/2)^2} \tag{7}$$

The full width Γ at half-maximum of the Lorentzian line profile corresponds to the damping constant of the acoustic power. The decaying acoustic signal recorded with the microphone is analyzed by a fast Fourier transform, and the resonances identified in the power spectrum are analyzed in respect to their line centers ω_0 and full widths at half-maximum Γ (see Fig. 5).

Experimental Results

Experimental Data from Hot-Fire Tests in the Common Research Chamber

Figure 6a shows a spectrogram of the acoustic response of the CRC to excitation by combustion noise. In this experiment, the combustion chamber was cylindrical, with no lateral cavity. The figure shows the spectrogram of the signal from a pressure probe placed at 180 deg with respect to the injector. The global equivalence ratio was 0.55 and the mean chamber pressure was 5 bar. The first second of the run is perturbed by the ignition transient. The low-frequency noise below 250 Hz is nonresonant turbulence-induced

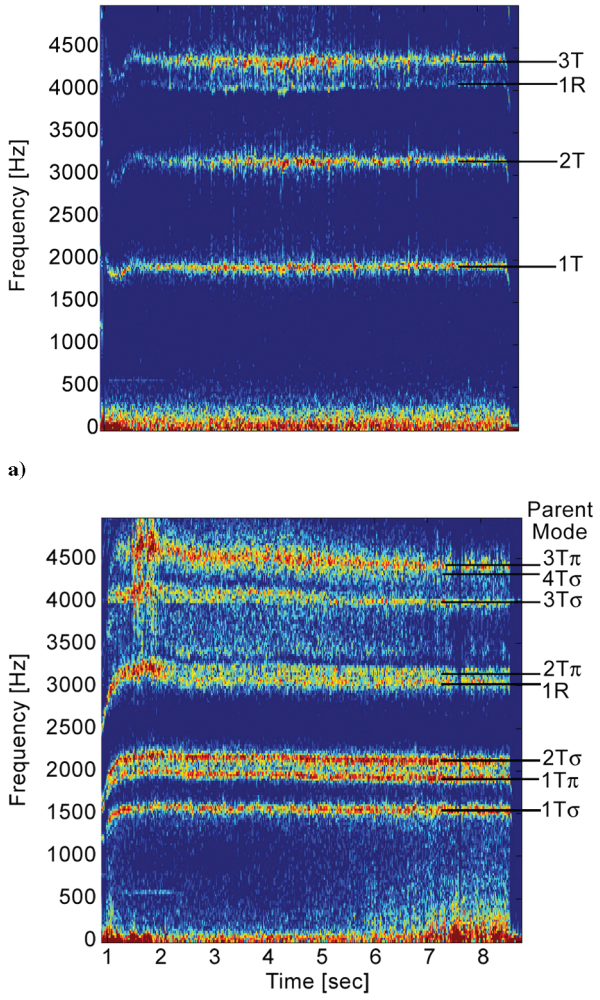

Fig. 6 Spectrogram of combustion noise: a) in CRC with no lateral cavity; b) with a lateral cavity placed at 135 deg with respect to the injector.

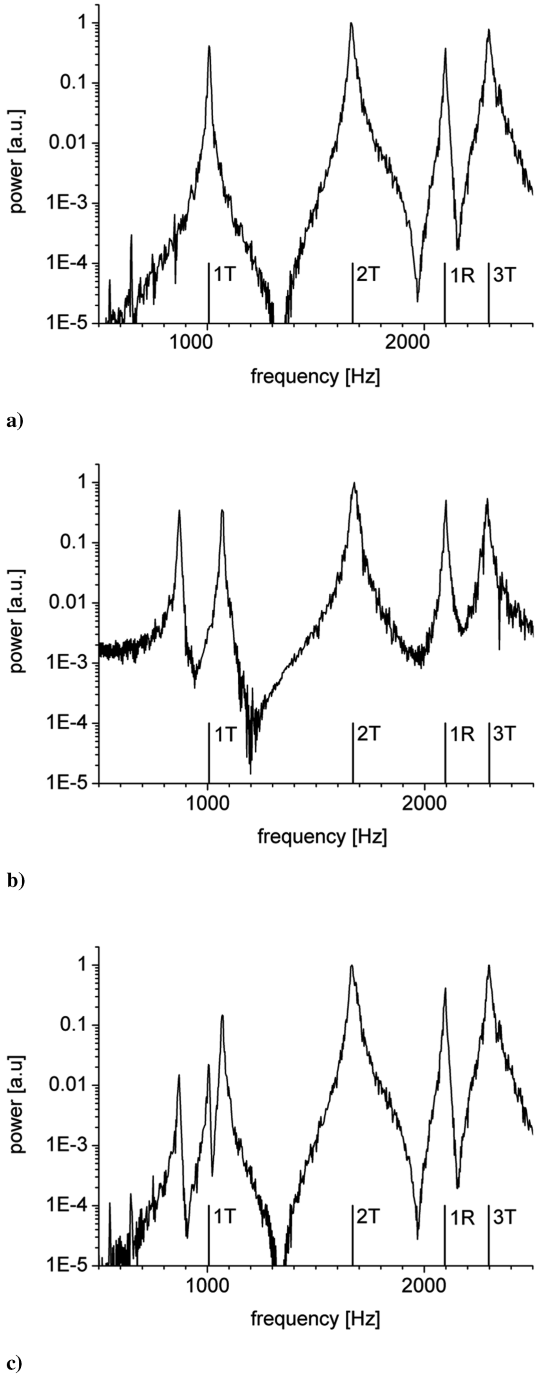

Fig. 7 Resonances of the CRC: a) without absorber, b) with absorber of length $L/R = 0.85$ and $\alpha = 0$ deg, and c) with absorber of length $L/R = 0.85$ and $\alpha = 22.5$ deg.

combustion noise. Three resonances are clearly visible. They correspond to the first, second, and third transverse modes (1T, 2T, 3T) of the cylindrical chamber. The theoretical frequencies of these modes are indicated for an assumed mean sound speed of 657 m/s. A weaker fourth resonance is also visible, just below the 3T resonance. Its frequency is that of the first radial mode of the chamber (1R).

When one of the CRC ports was replaced by the secondary nozzle, forming a lateral cavity as shown in Fig. 1, it was found that the mode frequencies changed substantially, with the appearance of extra resonances. Figure 6b shows a spectrogram taken under similar operating conditions, but with a lateral cavity of length $L = 82$ mm. The pressure sensor used here was placed adjacent to the cavity ($\alpha = 22.5$ deg). In place of the 1T resonance, there are now three resonances. The center resonance has the same frequency as the 1T mode of the CRC with no cavity. In anticipation of the analysis presented next, it is labeled 1Tπ. Its frequency is independent of the cavity length, but its amplitude goes to zero when the measurement position is placed diametrically opposite to the cavity ($\alpha = 180$ deg). The two adjacent resonances are labeled 1Tσ and 2Tσ. Their frequencies decrease as the cavity length is increased. It will be seen later that their frequencies tend to those of the 1T and 2T cylindrical modes as the length of the cavity tends to zero.

Experimental Data from Cold-Flow Tests in the Common Research Chamber

The spectral resolution that can be obtained in cold-flow tests with excitation by a loudspeaker with a well-controlled signal is superior to that from hot-fire tests. Therefore, the basic phenomenology of the acoustic resonances found in the CRC equipped with a secondary nozzle and excitation by combustion noise or siren wheel has been reproduced in cold-flow tests with excitation by a loudspeaker for quantitative analysis. The secondary nozzle has been replaced by a lateral cavity resembling a quarter-wave absorber in these tests.

Resonance spectra obtained with white noise excitation of the CRC without and with an absorber are shown in Figs. 7. As shown in Fig. 7a, without absorber, the measured resonance frequencies are in excellent agreement with the frequencies calculated for a cylindrical resonator.

Mounting a quarter-wave tube tuned to the 1T resonance ($L/R = 0.853$) changes the spectrum in a characteristic way. As can be seen in Fig. 7b, instead of the 1T resonance peak, two peaks appear with one peak at a frequency slightly below, and the other peak slightly above, the 1T resonance frequency. For this measurement,

the microphone was mounted on the symmetry line, as sketched in Fig. 3a. When the microphone position is rotated by $\alpha = 22.5$ deg relative to the symmetry axis, a third resonance peak appears at exactly the 1T resonance frequency (see Fig. 7c). The phenomenology is similar to that observed in the hot-fire tests reported in the preceding section, in which the CRC with a secondary nozzle is excited by combustion noise (see Fig. 6b). The resonances of a cylindrical chamber are changed in a characteristic way when a secondary cavity is coupled to the main chamber, even though the relative volume (0.82%) and cross section of the cavity are small.

In the next section, we will show that the basic phenomenology can be understood by studying two coupled resonators with a simple analytical model. However, quantitative prediction of the eigenfrequencies of coupled acoustic systems with complex geometries requires a numerical modal analysis.

Analysis of Eigenmodes and Eigenfrequencies

Analytical One-Dimensional Model of Coupled Resonators

To gain physical insight into the behavior of coupled resonators, we first present an analytical calculation of the resonant frequencies of two cavities with a common section. To make the calculation analytically tractable, we use a two-dimensional rectangular geometry in place of the cylindrical geometry of the CRC. We will also use a quasi-one-dimensional approximation, imposing that both pressure and the one-dimensional mass flux are continuous between the two cavities. The results of this analysis will not be quantitatively correct for the CRC, but we will expect that they are qualitatively correct and can serve as a guideline for understanding.

Formulation of the Problem

Consider two acoustic cavities of lengths L_1 and L_2, having cross sections A_1 and A_2, respectively. For convenience, we will suppose $A_1 > A_2$. The two cavities are coupled through a common face located at $x = 0$ (see Fig. 8). In each cavity, we suppose that there are two one-dimensional acoustic waves, one propagating to the right and the other to the left. The boundary conditions will then allow us to find the conditions of acoustic resonance.

Neglecting damping, we can write

$$p_{1,2} = (a_{1,2}e^{ikx} + b_{1,2}e^{-ikx})e^{i\omega t} \tag{8}$$

$$u_{1,2} = -\frac{1}{\rho c}(a_{1,2}e^{ikx} - b_{1,2}e^{-ikx})e^{i\omega t} \tag{9}$$

where $p_{1,2}$ are the acoustic pressures, $u_{1,2}$ are the acoustic velocities in cavities 1 and 2, respectively, k is the wave number, ω is the angular frequency, c is the speed of sound $c \equiv \omega/k$, and ρ is the mean density. The four constants to be determined are $a_{1,2}$ and $b_{1,2}$.

Boundary Conditions

The cavities are closed, and so the gas velocity is zero at the two extremities:

$$a_1 e^{-ikL_1} - b_1 e^{+ikL_1} = 0 \tag{10}$$

$$a_2 e^{+ikL_2} - b_2 e^{-ikL_2} = 0 \tag{11}$$

The pressure is continuous at the junction of the two cavities:

$$a_1 + b_1 = a_2 + b_2 \tag{12}$$

and we suppose that the one-dimensional mass flux is conserved at the junction:

$$A_1(a_1 - b_1) = A_2(a_2 - b_2) \tag{13}$$

The constants a_1 and a_2 can be eliminated in Eq. (12) with the help of Eqs. (10) and (11)

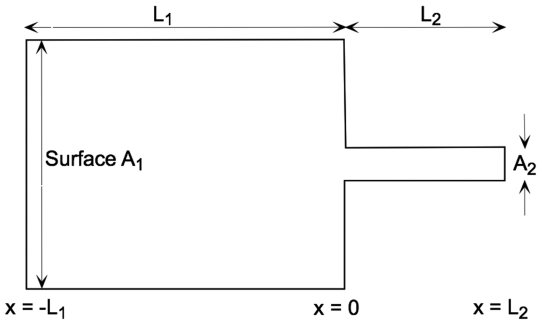

Fig. 8 Two acoustic cavities coupled at $x = 0$.

$$\frac{b_1}{b_2} = \frac{e^{-2ikL_2} + 1}{e^{+2ikL_1} + 1} \tag{14}$$

Similarly, a_1 and a_2 can be eliminated in Eq. (13):

$$\frac{b_1}{b_2} = \frac{A_2}{A_1}\frac{e^{-2ikL_2} - 1}{e^{+2ikL_1} - 1} \tag{15}$$

Solution

We will now look for the wave numbers that satisfy the boundary conditions. This is done by noticing that the right-hand side of Eqs. (14) and (15) must be equal. Rearranging yields

$$\tan(kL_1) = -\frac{A_2}{A_1}\tan(kL_2) \tag{16}$$

To simplify the notation, we will consider that the first cavity is the main cavity (combustion chamber) and that the second is a secondary cavity which perturbs the first cavity. We then renormalize using the following change of variables:

$$S = A_2/A_1 \quad 0 < S < 1$$

$$T = L_2/L_1 \quad \text{(unconditionally)}$$

$$F = kL_1/\pi \quad \text{(normalized frequency)}$$

F is now the global resonant frequency, normalized by the resonant frequency of the unperturbed main chamber, T is the relative length of the secondary cavity, and S is the ratio of the cross section of the secondary cavity to the main cavity. In the absence of the secondary cavity, the resonant frequencies are thus given by $F = 1, 2, 3, \ldots$. The condition of resonance for the two coupled cavities can then be written

$$F = \frac{1}{\pi}\tan^{-1}[-S\tan(\pi TF)] \tag{17}$$

Analysis of the Quasi-One-Dimensional Solution

Figure 9 shows the solutions to Eq. (17) as a function of the length ratio T, and for two ratios of cross section S. The value $S = 0.2$ is close to the effective value appropriate for the CRC and its lateral cavity.

When the length of the secondary cavity is equal to zero, we obtain the resonant frequencies $F = 1, 2, 3, \ldots$ of the classical $n\lambda/2$ modes of the main chamber. As T increases, the frequencies of the fundamental mode and the harmonics decrease, but the decrease in frequency is *not* linear with the length of the secondary cavity. The nonlinearity depends on the area ratio. When the ratio of cross sections is very small, we find that the resonances of the main chamber at $F = 1, 2, 3, \ldots$ are only weakly perturbed, with short fast transitions linking the main resonances. When the ratio of cross

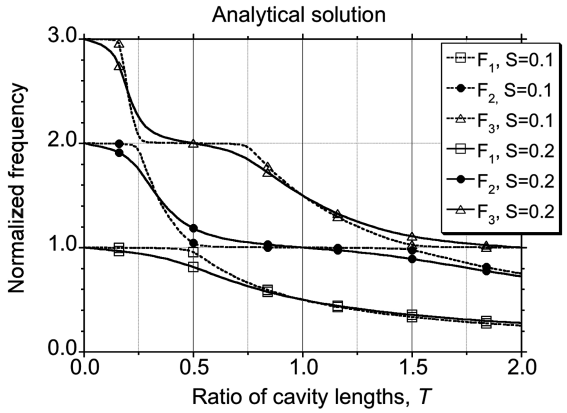

Fig. 9 Resonant frequencies of the double cavity as a function of damping cavity length, for two ratios of cross sections, $S = 0.1$ and $S = 0.2$.

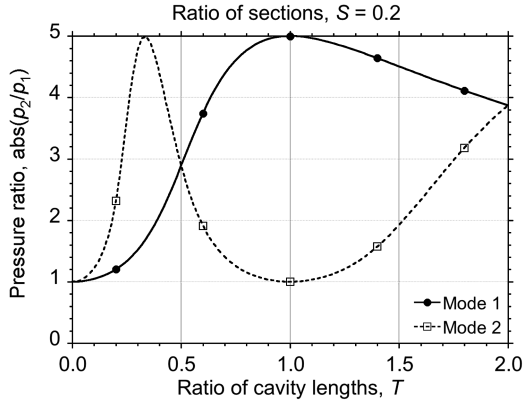

Fig. 10 Relative amplitude of the acoustic pressure in the lateral cavity ($x = L_2$) compared with the amplitude in the main chamber ($x = -L_1$) as a function of T.

sections is close to unity, the solutions tend toward those of a single cavity of length $L_1 + L_2$.

When $T = 0.5$, in other words, when the length of the secondary cavity is such that the frequency of its (isolated) $\lambda/4$ mode is equal to the fundamental frequency of the main chamber, we see that the coupled system has a pair of resonant frequencies placed, respectively, above and below the unperturbed resonant frequency 1. The lowest frequency stems from the fundamental mode of the main chamber, and the second resonance stems from the first harmonic of the main chamber. The frequencies of these two resonances become closer as the cross section of the damping cavity is decreased. This "double" resonance, centered at the fundamental frequency of the combustion chamber, is in qualitative agreement with our observations on the CRC.

When the acoustic lengths of the two cavities are equal, $T = 1$, the first two resonances of the coupled system have normalized frequencies $F = 0.5$ and $F = 1$. The first resonance is thus a mode with a half-wavelength in the double cavity, $\lambda/2 = L_1 + L_2$. The next resonance, at $F = 1$, is a mode with a half-wavelength in each cavity. The frequency of the "double $\lambda/2$" mode is relatively insensitive to the length of the secondary cavity when the ratio of sections is small.

We have neglected the damping of the system, and we have supposed that the gas flow is quasi-one-dimensional, even in the region of the change in section. In this approximation, we cannot calculate the shape of the resonance curves; however, we can obtain an indication of the relative amplitudes of the acoustic modes in each subcavity. To do this, we calculate the ratio of the acoustic pressure at the two extremities, $p_2(x = L_2)/p_1(x = -L_1)$:

$$\frac{p_2(x = L_2)}{p_1(x = -L_1)} = \frac{\cos(\pi F)}{\cos(\pi T F)} \tag{18}$$

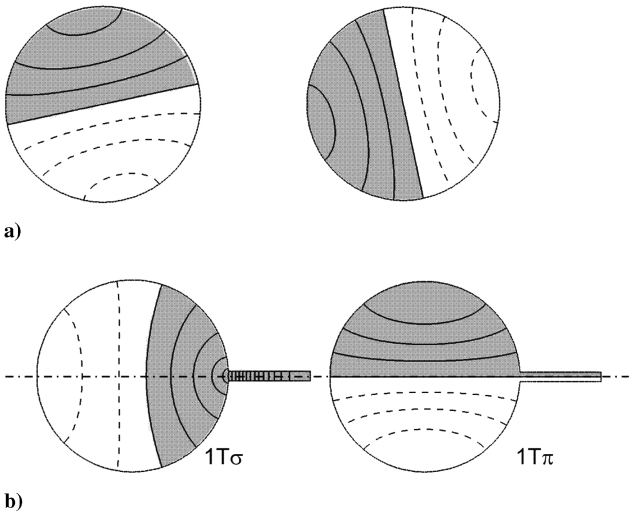

Fig. 11 Pressure distribution of eigenmodes: a) two degenerate 1T eigenmodes for a cylindrical resonator, and b) 1Tσ and 1Tπ mode for a cylindrical resonator with an absorber cavity of length $L/R = 0.85$.

This pressure ratio is plotted in Fig. 10 for a cross section ratio $S = 0.2$. The pressure ratio is calculated for the first two resonances, F_1 and F_2. It can be seen that the acoustic pressure in the cavity is always greater than the acoustic pressure in the main chamber. The strongest excitation of the lateral cavity does not occur when the cavity length is $\lambda/4$ ($T = 0.5$). For mode 1, the strongest excitation occurs for $T = 1$. We can infer that optimal mode 1 cavity damping will occur when the damping cavity is close to this length. For mode 2, the strongest excitation occurs for $T = 0.33$. Again, we expect that mode 2 damping will be most efficient for a cavity close to this length.

In the quasi-one-dimensional approximation, there is a simple analytical solution for the mode structure of two coupled rectangular cavities. The presence of a damping cavity has a strong effect on the mode structure in the main cavity. The resonant frequencies of the coupled system are different to those of the main chamber, and depend on both the length and diameter of the damping cavity. If the ratio of cross sections is small, the eigenfrequencies of the system vary very nonlinearly with the length of the damping cavity. The fast-changing frequencies occur when the length of the damping cavity is $n\lambda/4$ at the frequency of one of the resonances of the isolated main chamber. These analytical predictions are in qualitative agreement with the observation on our cylindrical combustion chamber. This analysis also suggests that the strongest damping will not be obtained when the damping cavity is tuned to this length. We now turn to numerical modeling to analyze the acoustics of more realistic geometries.

Numerical Modeling

Although the one-dimensional model explains the presence of the two peaks near the 1T resonance frequency when an absorber is coupled to the cylindrical combustor (see Fig. 7b), the appearance of the third component when the microphone is mounted at $\alpha =$ 22.5 deg (see Fig. 7c) can only be understood with a modal analysis that takes into account the full symmetry of the resonance volume, which can not represented in one dimension. The software FlexPDE has been used for two- and three-dimensional modal analysis of the problem. The eigenfrequencies and pressure fields of the eigenmodes have been determined for a cylindrical combustor of radius R equipped with an absorber of length L.

For the case of a pure cylindrical geometry, this modal analysis delivers two degenerate but independent solutions for each tangential eigenmode. For example, there are two 1T modes with identical eigenfrequency, whose pressure nodal lines are perpendicular to each other (see Fig. 11a). Because of the rotational symmetry of the resonance volume, there is no preferred orientation of the pressure nodes.

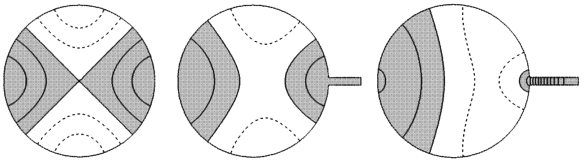

Fig. 12 Eigenmode 2Tσ for a cylindrical resonator a) without and with an absorber cavity of lengths b) $L/R = 0.43$ and c) $L/R = 0.64$.

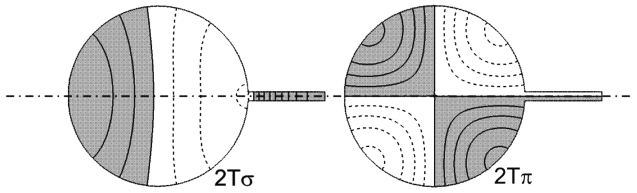

Fig. 13 Eigenmodes 2Tσ and 2Tπ for a cylindrical resonator with an absorber cavity of length $L/R = 0.85$.

When an absorber cavity is coupled to the cylinder, the rotational symmetry is broken. The resonance volume is now symmetric with respect to reflection about the symmetry line defined by the axis of the absorber, as shown in Fig. 11b. As a result of the reduced symmetry, the tangential modes are no longer degenerate and the orientation of the nodal line is now controlled by the orientation of the absorber. The modes having 1T symmetry change into the modes shown in Fig. 11b. One component now has its pressure nodal line perpendicular to the symmetry axis and the other component has its nodal line along the symmetry axis. The two modes now have different symmetry properties: one mode is symmetric with respect to reflection at the symmetry line, the other mode is antisymmetric. The labels σ (symmetric) and π (antisymmetric) are used to reflect this symmetry property.

The addition of an absorber also fixes the orientation of the nodal lines of the 2T (and higher) modes. Similar to the case of the 1T modes, the 2T modes split into σ and π components. Figure 12 shows the pressure distribution of the 2Tσ modes for several values of L/R. Although the basic symmetry of the 1T modes are conserved when an absorber is attached to the cylinder, such is not the case for the 2T mode. In contrast to the 1Tσ mode, the symmetry of the 2Tσ mode changes significantly when an absorber is added, as can be seen in Fig. 12. The two nodal lines of the 2T mode, which cross each other (Fig. 12a), become separated for the 2Tσ mode (Figs. 12b and 12c). With increasing absorber length, the symmetry of the 2Tσ mode in the cylinder resembles that of a 1T mode, as can be seen in Fig. 13. Note that there is a peculiar difference at the absorber inlet, which is important in respect to the absorber performance: the 2Tσ mode can have a nodal line in the vicinity of the absorber inlet, whereas the 1Tσ mode does not.

The evolution of the eigenfrequencies of the CRC equipped with an absorber of increasing length L is shown in Fig. 14. In general, the two-dimensional modal analysis shows a similar behavior, for the dependence of the eigenfrequencies on absorber length, to that found in the one-dimensional model (see Fig. 9). However, the one-dimensional model cannot predict the existence of the 1Tπ mode. For this mode, the pressure nodal line is in the absorber cavity, and hence the mode does not induce any significant fluid motion in the cavity. The 1Tπ resonance frequency is thus almost independent of the cavity length for realistic absorber diameters. The numerical predictions for eigenfrequencies of the CRC and cavity are in excellent agreement with the experimental data, such as shown later.

The experimental results in Figs. 7b and 7c can now be understood with the help of Fig. 14. For an absorber length of $L/R = 0.85$, three resonances are found near to the 1T frequency. They belong to the 1Tσ, 1Tπ, and 2Tσ modes. When the loudspeaker and microphone are mounted on the symmetry axis ($\alpha = 0$), the 1Tπ mode can neither

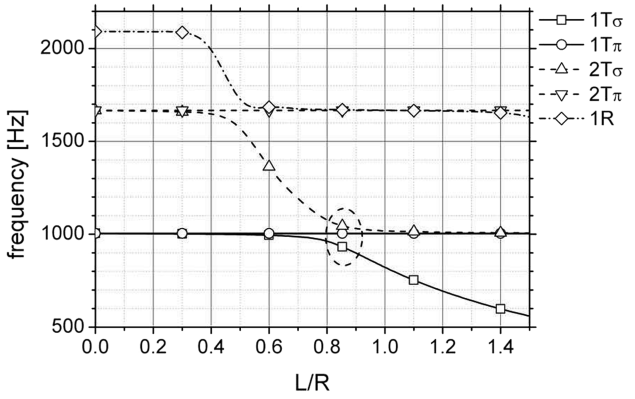

Fig. 14 Eigenfrequencies for a cylindrical resonator with an absorber cavity as function of the absorber length.

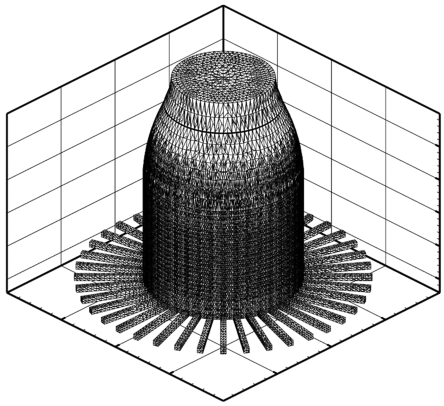

Fig. 15 Mesh for the modal analysis of a rocket combustor with a ring of 40 absorbers.

be excited nor detected because the loudspeaker and microphone are located on its pressure nodal line. Thus, in Fig. 7b, only the 1Tσ and 2Tσ modes are observed. When $\alpha = 22.5$ deg, all three modes are excited and the 1Tσ, 1Tπ, and 2Tπ resonances are seen in Fig. 7c.

For values of L/R as high as 0.85, the classification of modes according to the symmetries of the modes in the limit $L/R \to 0$ becomes questionable. The 2Tσ mode no longer has the 2T symmetry, as discussed earlier (see Fig. 13). In fact, for $L/R \sim 0.85$, the 2Tσ mode has 1T symmetry in the cylinder, and its resonance frequency is near to the 1T frequency. In this situation, the notation $1T^-$ and $1T^+$ for the 1Tσ and to the 2Tσ modes, which have their frequencies slightly below and above the 1T resonance frequency, respectively, may be better suited to indicate the main characteristics of these modes.

The analysis of a cylindrical resonator with an absorber tube has shown that the eigenfrequency of the coupled acoustic system deviates substantially from that of the cylindrical volume alone. In respect to the application of absorber rings to rocket chambers, we may ask whether a complete absorber ring detunes the system in a similar way to the simple system described earlier. We have performed a preliminary three-dimensional modal analysis of the eigenfrequencies of a volume representative of a rocket combustion chamber equipped with an absorber ring of 40 cavities. A sketch of the mesh is shown in Fig. 15. For this analysis, it has been assumed that the chamber is filled with ambient air. The nozzle is treated as acoustically closed. The results for the lowest eigenmodes are shown in Fig. 16. The dotted lines show the $\lambda/4$ resonant frequency of an isolated cavity, and also the length at which this $\lambda/4$ frequency is equal to 1T frequency of the main chamber. The eigenmodes with symmetries 1T, 2T, 3T, 4T, and 1R in the $L \to 0$ limit and the 1L mode have been analyzed. These modes all have a resonant frequency which decrease with increasing absorber length. Thus, an absorber ring detunes the spectrum of a rocket combustor

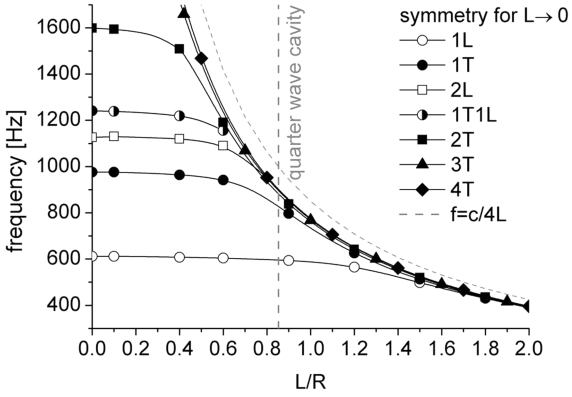

Fig. 16 Eigenfrequencies of the lowest eigenmodes of a rocket combustor with absorber ring.

significantly and its eigenspectrum differs from that of a cylindrical volume.

Damping of Acoustic Excitations

Experimental Data

The damping coefficients of the CRC with one absorber are obtained from the measurement of the linewidth Γ as explained earlier. The absorber used had a diameter of 12.4 mm. The data are plotted as a function of the absorber length for the 1T, 2T, and 1R modes in Fig. 17. The accuracy of the damping coefficients was about 1% for the CRC without absorber. For absorber lengths where high damping values were obtained, the signals become small and the uncertainty may increase up to more than 20%.

The quarter-wave resonance frequency $f_{QW} = c/4L$ of the absorber is plotted in Figs. 17a–17c as dashed lines. Apparently, high damping is observed for the individual modes when the absorber length is such that the eigenfrequencies of the coupled acoustic system have a resonance frequency close to the quarter-wave resonance of the absorber.

The dash-dotted lines in Fig. 17 mark the lengths where a quarter-wave resonator would be tuned to the frequency of one of the cylinder modes [see Eq. (3)]. For the 1T, 2T, and 1R modes, the values of L/R are 0.85, 0.51, and 0.37, respectively. Figure 17 shows that maximum damping is obtained near, but not exactly at, these lengths. Maximum damping is measured for the 1T and 1R modes for an absorber length about 10% longer than predicted by simple quarter-wave theory. For the 2T mode, two maxima are observed, with the highest damping value obtained for an absorber whose length is 40% larger than predicted by quarter-wave theory.

It is interesting to evaluate the length range over which an absorber shows good damping. This should give an indication of the sensitivity of damping behavior to cavity length adjustment. For the 1T mode, a variation of L/R from 0.86 to 1.01 does not result in a decrease of the damping below 90% of its maximum value. For the 2T mode, maximum damping occurs for $L/R = 0.71$. But, again, the damping is high for a range of absorber lengths and does not fall below 85% of its maximum value for L/R ranging from 0.44 to 0.75.

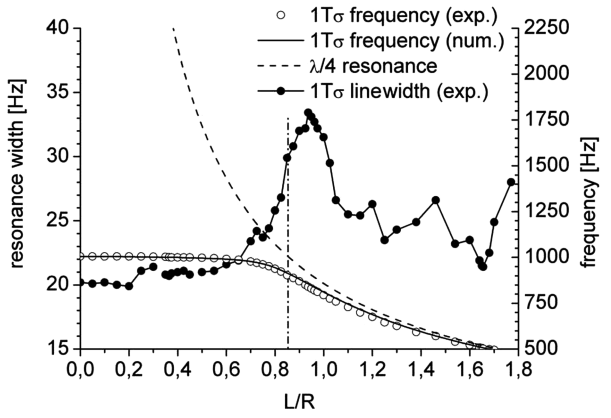

a)

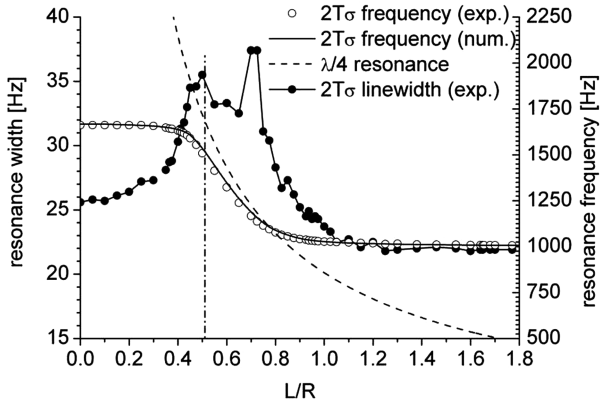

b)

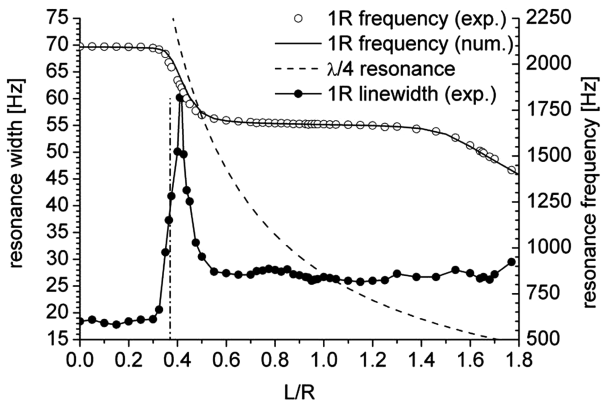

c)

Fig. 17 Damping coefficient and resonance frequency as function of the resonator length for a) 1Tσ resonance, b) 2Tσ resonance, and c) 1R resonance.

Numerical Modeling

Numerical modal analysis was performed to obtain the eigenfrequencies of the coupled acoustic system of combustor and absorber. It provides not only the frequencies, but also the pressure distribution $P(\mathbf{r})$ and the velocity field $\mathbf{u}(\mathbf{r}) = (i/\rho\omega)\nabla(P)$ of the eigenmodes. The damping processes by which the absorber contributes to the overall damping of the system are related to the velocity field. The objective here is to use this information for a qualitative discussion on how the absorber length influences the damping behavior. The approach does not aim to provide a quantitative estimation of damping constants, nor to replace a detailed investigation of basic physical processes, such as, for example, viscous and thermal dissipation in the boundary layers or vortex shedding at the absorber inlet.

The discussion is based on eigenmodes obtained from a two-dimensional analysis of the problem. The computational domain is a cylindrical combustor of area $A_c = \pi R^2$ and a rectangular absorber, as sketched, for example, in Fig. 13.

When streamlines of the acoustic velocity field enter the absorber, the flow is accelerated. A zoom of this region is shown in Fig. 18 for illustration. The acoustic boundary condition at the rear end of the absorber requires zero velocity, thus it can be assumed that the major contribution to the damping processes originates from the absorber inlet region. For this reason, the following analysis takes into account only the velocity at the absorber inlet. First, we define a quantity q

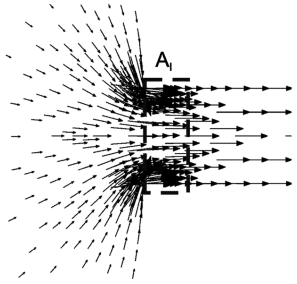

Fig. 18 Flowfield at the absorber inlet.

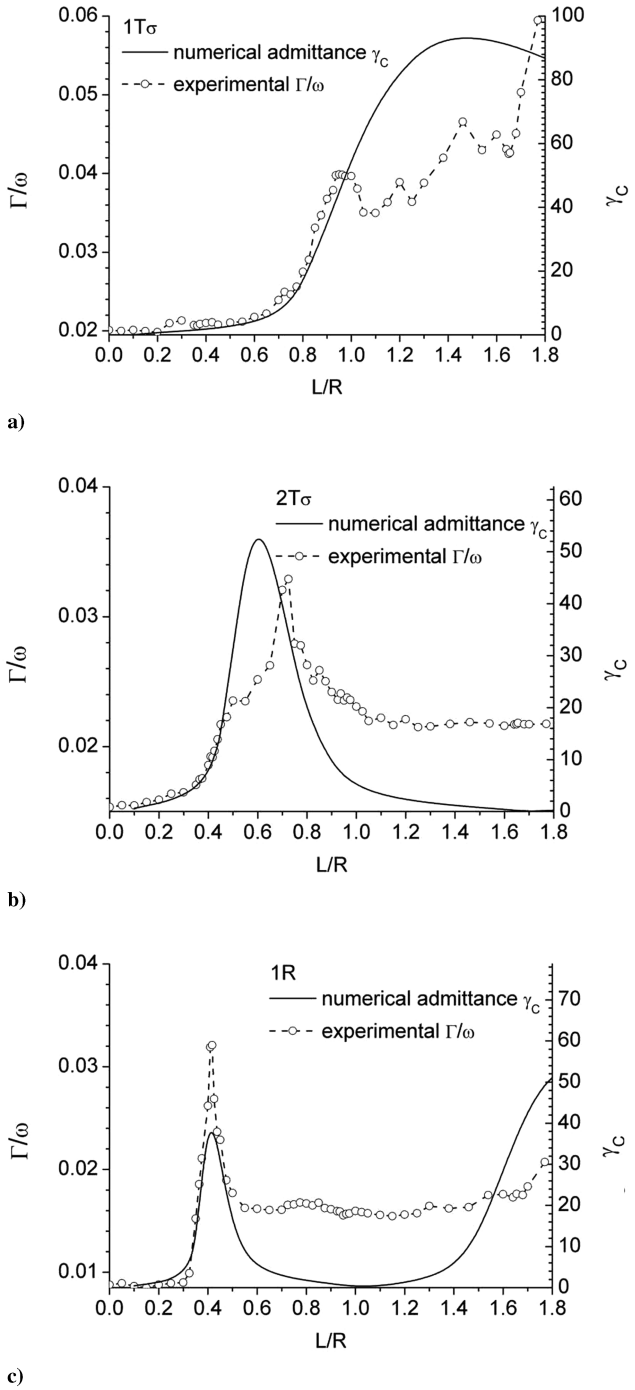

Fig. 19 Damping/period and admittance γ_c as function of the resonator length a) for 1T resonance, b) for 2T resonance, and c) for 1R resonance.

which, for a given eigenmode, is proportional to the mean value of the velocity in the absorber inlet area A_I (see Fig. 18):

$$q = \frac{c}{\omega} \int_{A_I} |\nabla P'| \, \mathrm{d}A / A_I \tag{19}$$

Next, the mean pressure level p_C of the eigenmode is determined in the computational domain representing the main combustor with the area A_C:

$$p_C = \int_{A_C} |P'| \, \mathrm{d}A / A_C \tag{20}$$

Finally, the quantity q is normalized by the value of the acoustic excitation p_C in the combustor:

$$\gamma_C = \frac{q}{p_C} \tag{21}$$

By this definition, γ_C represents the mean velocity at the absorber inlet when a mean acoustic excitation p_C is given in the combustor for the mode under investigation. The quantity γ_C is nondimensional and is defined in analogy to an absorber admittance.

The dependence of γ_C on the absorber length, for the eigenmodes 1T, 2T, and 1R, is shown in Fig. 19. For comparison, the experimentally determined nondimensional damping constants Γ/ω are also shown. The scales for γ_C and Γ/ω in Figs. 19a–19c have been adjusted in the same way for all three modes. The origins are shifted so that $\gamma_C = 0$ corresponds to the experimental damping value Γ/ω for a combustor without absorber ($L/R = 0$).

Taking into account the simplicity of the model used to define the admittance γ_C, the similarity with the measured data is surprisingly good for all modes investigated. The admittance γ_C predicts the increase of damping with increasing absorber length very well. For small values of L/R, the evolution of γ_C and Γ/ω with increasing absorber length are almost identical. For the 2T and 1R modes, the lengths at which maximum damping is obtained is also predicted reasonably. There is a general qualitative agreement concerning the absorber lengths where damping increases and decreases.

However, there are significant differences demonstrating the limitations of the concept of γ_C. For absorber lengths where the experimental damping is high, the agreement between γ_C and Γ/ω is not good. In this region, there is no mode for which γ_C predicts the dependence of Γ/ω on absorber length well. Also, for large values of L/R, the good agreement between γ_C and Γ/ω observed for small values of L/R is not found.

Summary and Conclusions

In combustion experiments and in combustors filled with ambient air, it has been shown that the presence of an absorber cavity has significant influence on the acoustic eigenmodes of the coupled acoustic system composed of the combustor and cavity. The eigenmodes of the coupled system are not identical to the eigenmodes of the combustor without absorber. The resonance frequencies of all modes are shifted to lower values with increasing absorber length. Also, due to the loss of rotational symmetry in the presence of an absorber, the degeneracy of the tangential modes is broken. Thus, new resonances appear in the spectrum of eigenfrequencies. A profound change in the symmetry properties of the modes is associated with the change of the resonance frequencies. The general phenomenology can be well understood by studying a simplified analytical model for the coupled acoustic system of an absorber and a combustor. However, the quantitative prediction of resonance frequencies necessitates the use of numerical modal analysis, which can take into account the full complex geometry of the problem.

The contribution of an absorber to the damping of acoustic excitations has been determined experimentally. Maximum damping is found to occur at larger absorber lengths than that predicted by simple quarter-wave theory. A qualitative discussion of the damping behavior, based on the acoustic velocity field of the eigenmodes,

shows partial agreement with experimental data. This gives an indication of the potential to extract information on the damping behavior in resonators of complex geometries based on the acoustic velocity fields of the eigenmodes.

From the results of the work presented here, which focuses on a single absorber coupled to a combustion chamber, it is concluded that the analysis should be extended to investigate the performance of absorber rings in rocket combustion chambers, a task which has been only superficially addressed in this paper.

References

[1] Harrje, D., and Reardon, F., "Liquid Propellant Rocket Combustion Instability," NASA SP-194, 1972.

[2] Yang, V., and Anderson, W. (eds.), *Liquid Rocket Engine Combustion Instability*, Progress in Astronautics and Aeronautics, AIAA, Washington, D.C., Vol. 169, 1995.

[3] Oefelein, J., and Yang, V., "Comprehensive Review of Liquid-Propellant Combustion Instabilities in F-1 Engines," *Journal of Propulsion and Power*, Vol. 9, No. 5, 1993, pp. 657–677.

[4] Bazarov, V., and Yang, V., "Liquid-Propellant Rocket Engine Injector Dynamics," *Journal of Propulsion and Power*, Vol. 14, No. 5, 1998, pp. 797–806.

[5] Cavitt, R., Frederick, R., and Bazarov, V., "Experimental Methodology for Measuring Combustion and Injection-Coupled Responses," *42nd Joint Propulsion Conference and Exhibit*, AIAA Paper 2006-4527, 2006.

[6] Oberg, C., Wong, T., and Ford, W., "Evaluation of Acoustic Cavities for Combustion Stabilization," NASA CR 115087, 1971.

[7] Laudien, E., Pongratz, R., Pierro, R., and Preclik, D., "Experimental Procedures Aiding the Design of Acoustic Cavities," *Liquid Rocket Engine Combustion Instability*, edited by V. Yang and W. Anderson, Progress in Astronautics and Aeronautics, Vol. 169, AIAA, Washington, D.C., 1995, pp. 377–399.

[8] Richards, G., Straub, D. L., and Robey, E., "Passive Control of Combustion Instabilities in Stationary Gas Turbines," *Combustion Instabilities in Gas Turbine Engines*, edited by T. Liuwen and V. Yang, Progress in Astronautics and Aeronautics, Vol. 210, AIAA, Reston, VA, 2005.

[9] Cheuret, F., "Instabilités Thermo-Acoustiques de Combustion Haute-Fréquence dans les Moteurs Fusées," Ph.D. Thesis, Univ. de Provence, Marseille, France, Oct. 2005, http://tel.archives-ouvertes.fr/tel-00011656.

[10] Heidmann, M., "Oscillatory Combustion of a Liquid-Oxygen Jet with Gaseous Hydrogen," NASA TN-D-2753, 1965.

[11] Alonso, M., and Finn, E., *Fundamental University Physics*, Addison-Wesley, Reading, MA, Vol. 1, 1967.

[12] Demtröder, W., *Laser Spectroscopy*, Springer, New York, 1996.

D. Talley
Associate Editor